Supporting Information

Qing-Xue Ma,[a] Cong-Cong Shu,[b] Jiao-Yang Qiao,[a] Cai-Xia Dong, *[c] and Zhong-Ming Sun*[a]

[a] State Key Laboratory of Elemento-Organic Chemistry, Tianjin Key Lab of Rare Earth Materials and Applications, School of Materials Science and Engineering, Nankai University, Tianjin 300350, China. E-mail:sunlab@nankai.edu.cn
[b] Department of Chemistry and Research Center for Chemical Biology and Omics Analysis, College of Science, Southern University of Science and Technology, Shenzhen 518055, China.
[c] College of Resources and Environmental Engineering, Inner Mongolia University of Technology, Hohhot, China. E-mail: dongcx@imut.edu.cn

Table of Contents

1. Experimental Procedures

All manipulations and reactions were performed under a nitrogen atmosphere using standard Schlenk or glovebox techniques. Ethylenediamine (en) (Aldrich, 99%) was freshly distilled by CaH_2 prior to use. The solvent toluene (tol) (Aldrich, 99.8%) was freshly distilled from sodium-benzophenone. Acetonitrile (Aldrich, 99.8%) was distilled from CaH_2 under N_2 and stored under nitrogen prior to use. 4,7,13,16,21,24-Hexaoxa-1,10-diazabicyclo[8.8.8]hexacosane ([2.2.2]-crypt, Sigma-Aldrich 98%) was dried under a vacuum for 12 hours prior to use. K_4Pb_9 was synthesized by heating a stoichiometric mixture of corresponding elements at 800 °C for two days in niobium tubes. (1,3-Bis(2,6-diisopropylphenyl)-1*H*-imidazol-2(3*H*)-ylidene)silver chloride was prepared according to modified literature procedures.[1] Chloro(triphenylphosphine)silver was prepared according to modified literature procedures.[2] Chloro(1,3-dimesitylimidazol-2-ylidene)copper(I) and 1,3-Bis(2,6-diisopropylphenyl)-2,3-dihydro-2-imidazolyl]copper(I) Chloride were purchased from Aldrich.

Synthesis of $[K([2.2.2]crypt)]_3[Ag@Pb_{12}]\cdot tol$ (1)

In a 10 ml vial, K_4Pb_9 (202 mg, 0.1 mmol) and 2.2.2-crypt (150 mg, 0.4 mmol) were dissolved in 3.0 ml en and stirred at room temperature for 0.5 h to yield a black–brown solution. (1,3-Bis(2,6-diisopropylphenyl)-1*H*-imidazol-2(3*H*)-ylidene)silver chloride (11.4 mg, 0.05 mmol) was added slowly to this mixture over 0.5 h and then stirred vigorously for 3.0 h. The mixture was centrifuged and the liquid supernatant transferred to a test tube, then carefully layered with toluene (3.0 ml) to allow for crystallization. After 5 days, block-like crystals of **1** were observed in the test tube with a yield of ~24% (based on Ag).

X-ray Diffraction:

The single crystal diffraction data was collected on Rigaku XtalAB PRO MM007 DW at 100 K, with a Hybrid Pixel Array CCD Detector. The X-ray source is Mo Kα ($\lambda = 0.7107$ Å). The raw diffraction data was collected and reduced by the program of "CrysAlisPro 1.171.40.84a (Rigaku OD, 2020)", and treated by multi-scan absorption correction. Using direct methods, we solved the structures and refined them to convergence using SHELXL-2014 and Olex2.[3-5] Non-hydrogen atoms were refined anisotropically, except for those in split positions, while all hydrogen atoms of organic groups were placed rationally using geometrical considerations.

Electrospray Ionization Mass Spectrometry (ESI-MS) Investigations:

ESI-MS analysis was conducted using an Agilent Technologies ESI-TOF-MS (6230) on an LTQ linear ion trap spectrometer. The spray voltage and capillary voltage were set to 5.48 kV and 30 V, respectively, while the capillary temperature was maintained at 300 °C.

Energy Dispersive X-ray (EDX) Spectroscopic Analysis:

We conducted EDX analysis with a scanning electron microscope (FE-SEM, JEOL JSM-7800F, Japan), using an acceleration voltage of 20 kV and an accumulation time of 150 s for data acquisition.

2. Crystallographic Supplementary Information

2.1 General

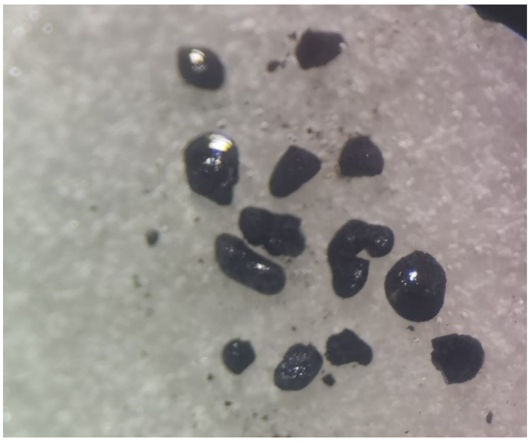

Figure S1. Block–like crystals for **$[K([2.2.2]crypt)]_3[Ag@Pb_{12}]\cdot tol$ (1)** dispersed in silicon oil.

Table S1. X-ray measurements and structure solutions of **[K([2.2.2]crypt)]$_3$[Ag@Pb$_{12}$]·tol (1)**.

compound	**1**
Empirical formula	$C_{75}H_{132}AgK_3N_6O_{18}Pb_{12}$
Formula weight	4117.31
Temperature/K	100.00(10)
Crystal system	trigonal
Space group	*R-3*
a/Å	24.9000(3)
b/Å	24.9000(3)
c/Å	29.8591(4)
α/°	90
β/°	90
γ/°	120
Volume/Å^3	16032.7(4)
Z	6
ρ_{calc}g/cm^3	2.559
μ/mm^{-1}	19.179
F(000)	10953.6
2Θ range for data collection/	4.02 to 68.14
Reflections collected/ unique	25209
Data/restraints/parameters	7563/0/348
Goodness-of-fit on F^2	1.032
Final R indexes [I>=2σ (I)]	R_1 = 0.0258, wR_2 = 0.0620
Final R indexes [all data]	R_1 = 0.0365, wR_2 = 0.0650
Largest diff. peak/hole / e Å^{-3}	2.86/-2.34
CCDC	2526890

[a] $R_1 = = \sum||F_o|-|F_c||/\sum|F_o|$; $wR_2 = \{\sum w[(F_o)^2-(F_c)^2]^2/\sum w[(F_o)^2]^2\}^{1/2}$

[b] GooF = $\{\sum w[(Fo)^2-(Fc)^2]^2/(n-p)\}^{1/2}$

2.2 Details of structure

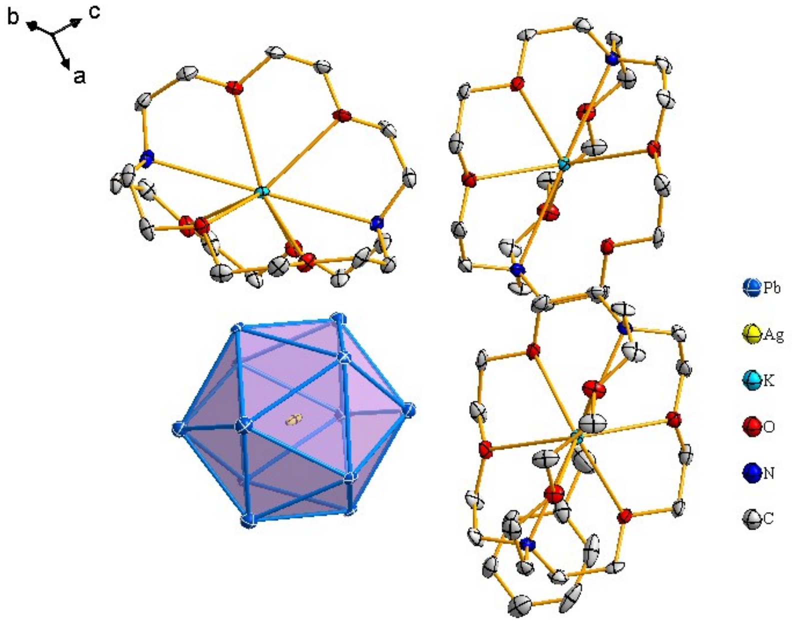

Figure S2. Asymmetric unit of **[K([2.2.2]crypt)]$_3$[Ag@Pb$_{12}$]·tol (1)** with the cluster fragment. Thermal ellipsoids are drawn at 50% probability. Hydrogen atoms are omitted for clarity.

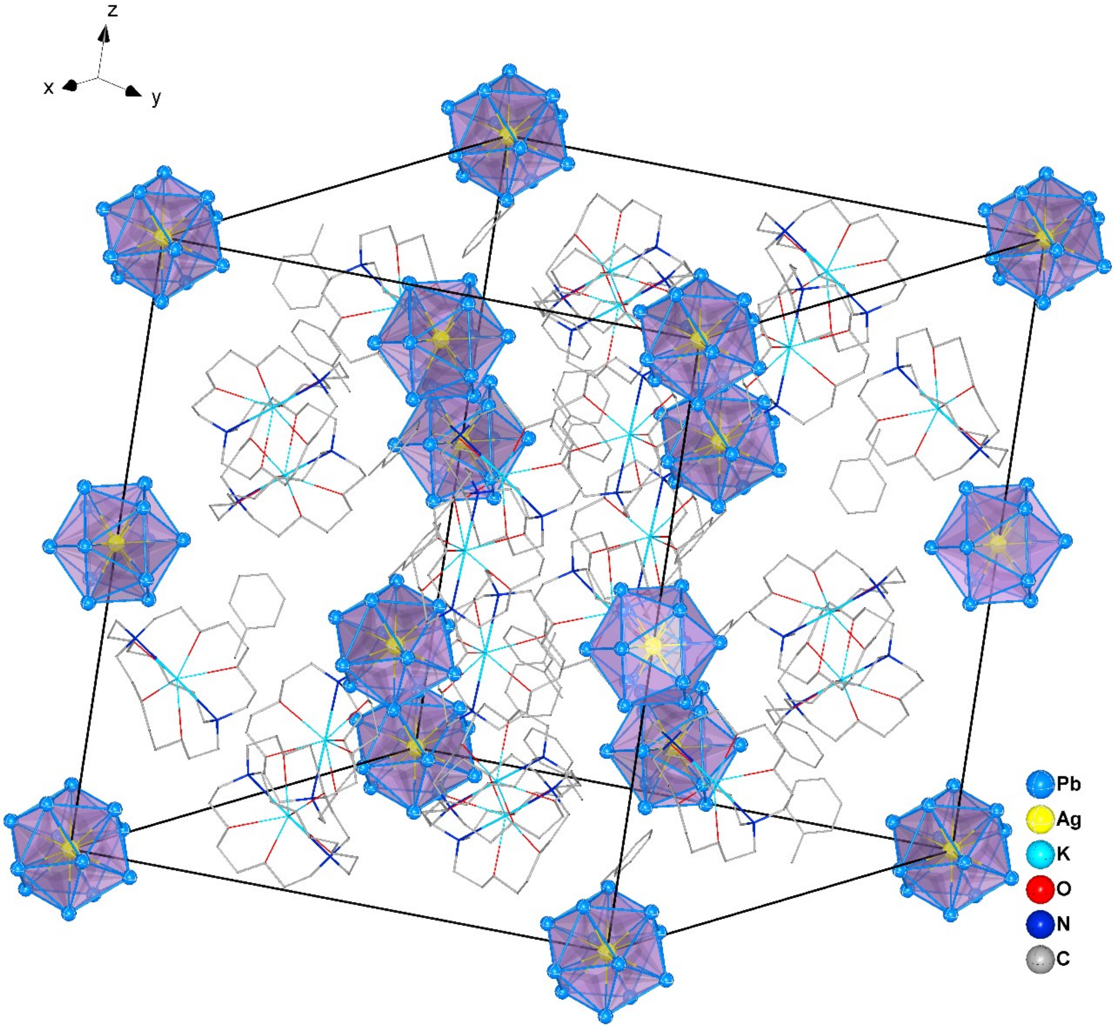

Figure S3. Unit cell of **[K([2.2.2]crypt)]$_3$[Ag@Pb$_{12}$]$_2$·tol (1)**. The disorder positions (atoms and bonds) and H atoms in the cluster are omitted for clarity.

2. ESI-MS Studies

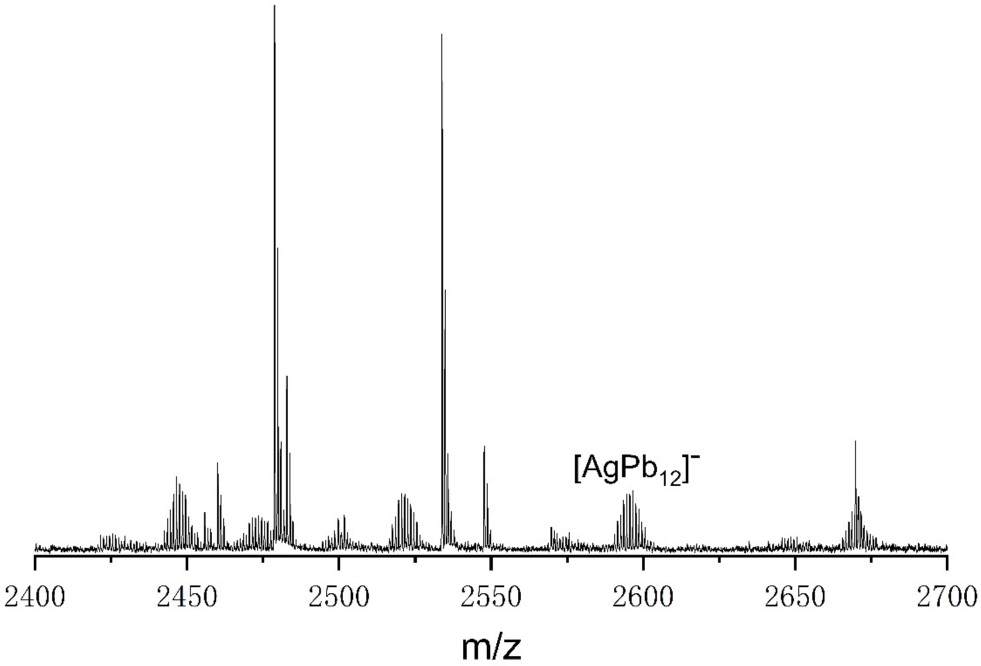

Figure S4. Overview of ESI–MS in negative ion mode of a freshly dissolved crystalline sample of **1** in acetonitrile.

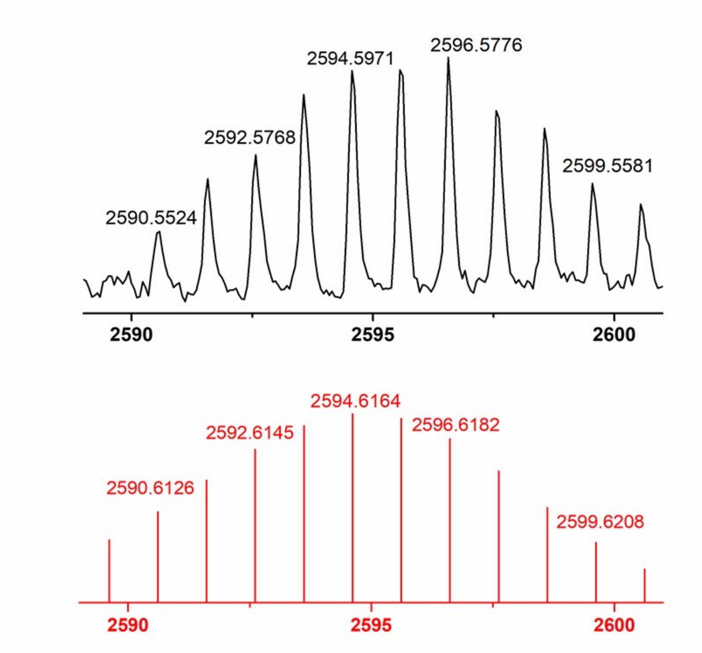

Figure S5. Measured (black) and simulated (red) spectra of the fragment [AgPb$_{12}$]$^-$.

3. EDX Studies

EDX analysis was carried out on **1** using a scanning electron microscope (FE-SEM, JEOL JSM-7800F, Japan). The acceleration voltage and accumulation time were 20 kV and 150 s, respectively. EDX analysis qualitatively confirms the presence of K, Ag, and Pb in the crystal of **K([2.2.2]crypt)]$_3$[Ag@Pb$_{12}$]·tol (1)**.

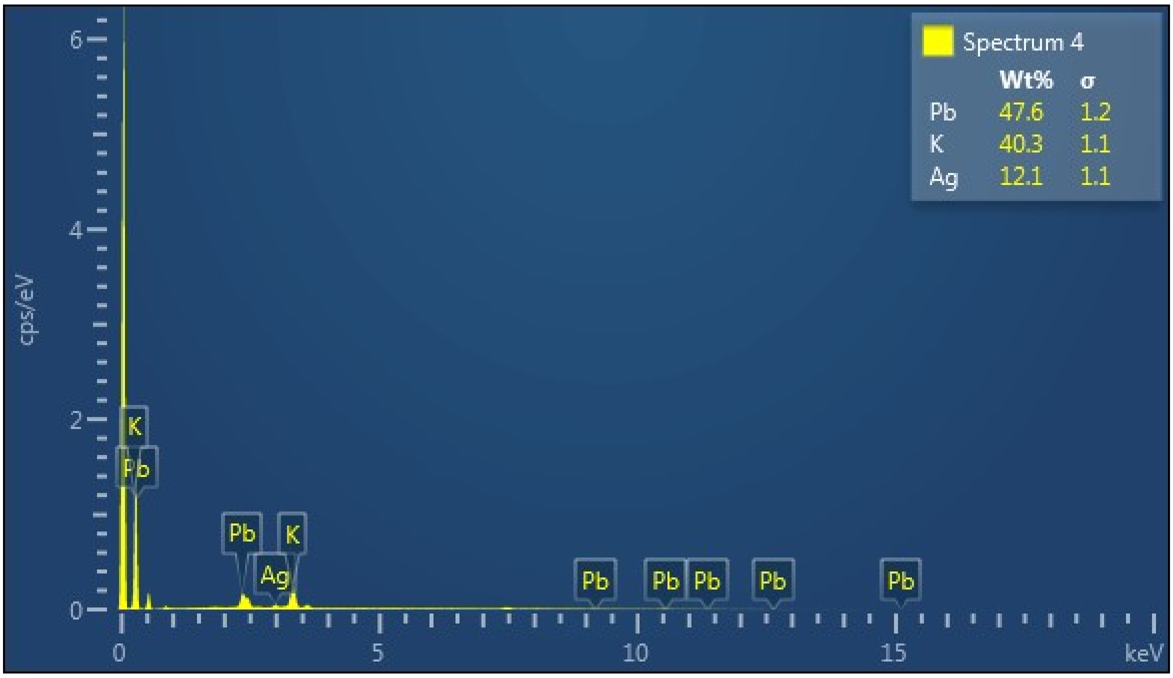

Figure S6. EDX analysis of complex **K([2.2.2]crypt)]$_3$[Ag@Pb$_{12}$]·tol (1)**.

4. Control Experiments

To investigate the role of the NHC ligand and the specificity of the metal center in the formation of the endohedral [M@Pb$_{12}$]$^{3-}$ cluster, we performed a series of control experiments under reaction conditions analogous to those used for the successful isolation of [Ag@Pb$_{12}$]$^{3-}$.

4.1 Attempted Synthesis Using a Phosphine-Stabilized Silver(I) Precursor

Reaction A: In a 10 ml vial, K$_4$Pb$_9$ (202 mg, 0.1 mmol) and 2.2.2-crypt (150 mg, 0.4 mmol) were dissolved in 3.0 ml en and stirred at room temperature for 0.5 h to yield a black–brown solution. Chloro(triphenylphosphine)silver (20.3 mg, 0.05 mmol) was added slowly to this mixture over 0.5 h and then stirred vigorously for 3.0 h. The mixture was centrifuged and the liquid supernatant transferred to a test tube, then carefully layered with toluene (3.0 ml) to allow for crystallization. After 5 days, block-like crystals of [K([2.2.2]crypt)]$_4$[Pb$_9$] were observed in the test tub.

4.2 Attempted Synthesis of the Copper Analogue [Cu@Pb$_{12}$]$^{3-}$

Reaction B: In a 10 ml vial, K$_4$Pb$_9$ (202 mg, 0.1 mmol) and 2.2.2-crypt (150 mg, 0.4 mmol) were dissolved in 3.0 ml en and stirred at room temperature for 0.5 h to yield a black–brown solution. 1,3-Bis(2,6-diisopropylphenyl)-2,3-dihydro-2-imidazolyl]copper(I) Chloride (IPrCuCl) (24.4 mg, 0.05 mmol) was added slowly to this mixture over 0.5 h and then stirred vigorously for 3.0 h. The mixture was centrifuged and the liquid supernatant transferred to a test tube, then carefully layered with toluene (3.0 ml) to allow for crystallization. After 5 days, block-like crystals of [K([2.2.2]crypt)]$_3$[Cu@Pb$_9$] were observed in the test tub.

Reaction C: In a 10 ml vial, K$_4$Pb$_9$ (202 mg, 0.1 mmol) and 2.2.2-crypt (150 mg, 0.4 mmol) were dissolved in 3.0 ml en and stirred at room temperature for 0.5 h to yield a black–brown solution. Chloro(1,3-dimesitylimidazol-2-ylidene)copper(I) (IMesCuCl) (20.1 mg, 0.05 mmol) was added slowly to this mixture over 0.5 h and then stirred vigorously for 3.0 h. The mixture was centrifuged and the liquid supernatant transferred to a test tube, then carefully layered with toluene (3.0 ml) to allow for crystallization. The reaction using IMesCuCl yielded only an amorphous, mud-like solid from which no crystalline product could be isolated, despite repeated crystallization attempts.

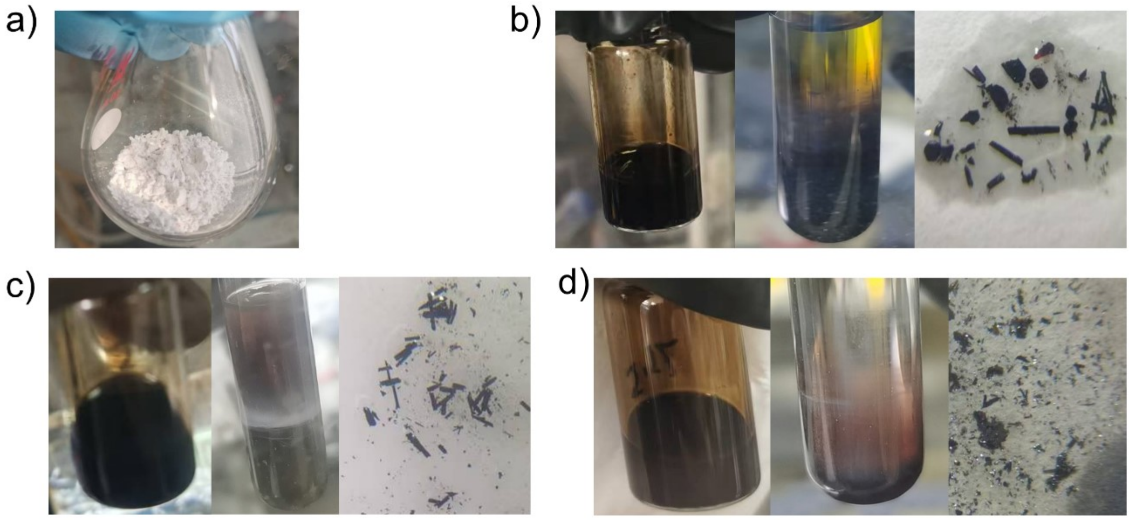

Figure S7. a) $AgPPh_3Cl$ b) reaction A and crystals of $[K([2.2.2]crypt)]_4[Pb_9]$ c) reaction B and crystals of $[K([2.2.2]crypt)]_3[Cu@Pb_9]$ c) reaction C and no crystalline product.

5. Computational Details

All quantum-chemical calculations were performed with Gaussian 09[6]. Geometry optimizations were carried out using the PBE0 hybrid functional[7] and the def2-TZVP basis set[8] , followed by subsequent electronic-structure calculations based on the optimized geometries. Harmonic vibrational frequency analyse was carried out for optimized ground-state structures to confirm its stability and to ensure that the structure corresponds to a true minimum on the potential energy surface (no imaginary frequencies). The solid-state confining effect of cations was simulated with the continuum solvent model (PCM) by setting the dielectric constant to $\varepsilon_r = 12.9$. The resulting wavefunction-derived properties and visualization outputs were analyzed using Multiwfn (v3.8)[9, 10], and molecular structures/orbitals were rendered with VMD (v1.9.3)[11].

Table S2. Energy and Cartesian coordinates (in Å) for the optimized $[Ag@Pb_{12}]^{3-}$ cluster.

$[Ag@Pb_{12}]^{3-}$	E: -67008.5014eV		
Pb	1.8091868042	1.0445345295	2.3466088734
Pb	-0.0000000517	3.0373936709	0.7893861193
Ag	0.0000000000	0.0000000000	0.0000000000
Pb	2.6304601062	-1.5186967907	0.7893861193
Pb	-1.8091868397	1.0445344679	2.3466088734
Pb	0.0000000355	-2.0890689973	-0.7893861193
Pb	-2.6304601062	1.5186967907	-0.7893861193
Pb	-0.0000000355	2.0890689973	-2.3466088734
Pb	-1.8091868042	-1.0445345295	-2.3466088734
Pb	1.8091868397	-1.0445344679	-2.3466088734
Pb	-2.6304600545	-1.5186968802	0.7893861193
Pb	0.0000000517	-3.0373936709	-0.7893861193
Pb	1.8091868042	1.0445345295	2.3466088734

Table S3. NPA valence electron configurations, charge (a.u.) for the $[\mathrm{Ag@Pb}_{12}]^{3-}$ clusters.

Species	**Electron configuration**	**Charge (a.u.)**
$[\mathrm{Ag@Pb}_{12}]^{3-}$		
Pb	6*s*(1.75)6*p*(2.44)6*d*(0.02)7*p*(0.01)	-0.21
Pb	6*s*(1.74)6*p*(2.38)6*d*(0.02)7*p*(0.01)	-0.14
Ag	5*s*(0.43)4*d*(9.90)5*p*(1.53)6*s*(0.03)6*p*(0.01)	-0.91
Pb	6*s*(1.74)6*p*(2.38)6*d*(0.02)7*p*(0.01)	-0.14
Pb	6*s*(1.75)6*p*(2.44)6*d*(0.02)7*p*(0.01	-0.21
Pb	6*s*(1.75)6*p*(2.44)6*d*(0.02)7*p*(0.01)	-0.21
Pb	6*s*(1.74)6*p*(2.38)6*d*(0.02)7*p*(0.01)	-0.14
Pb	6*s*(1.74)6*p*(2.38)6*d*(0.02)7*p*(0.01)	-0.14
Pb	6*s*(1.75)6*p*(2.44)6*d*(0.02)7*p*(0.01)	-0.21
Pb	6*s*(1.75)6*p*(2.44)6*d*(0.02)7*p*(0.01)	-0.21
Pb	6*s*(1.75)6*p*(2.44)6*d*(0.02)7*p*(0.01)	-0.21
Pb	6*s*(1.74)6*p*(2.38)6*d*(0.02)7*p*(0.01)	-0.14
Pb	6*s*(1.74)6*p*(2.38)6*d*(0.02)7*p*(0.01)	-0.14

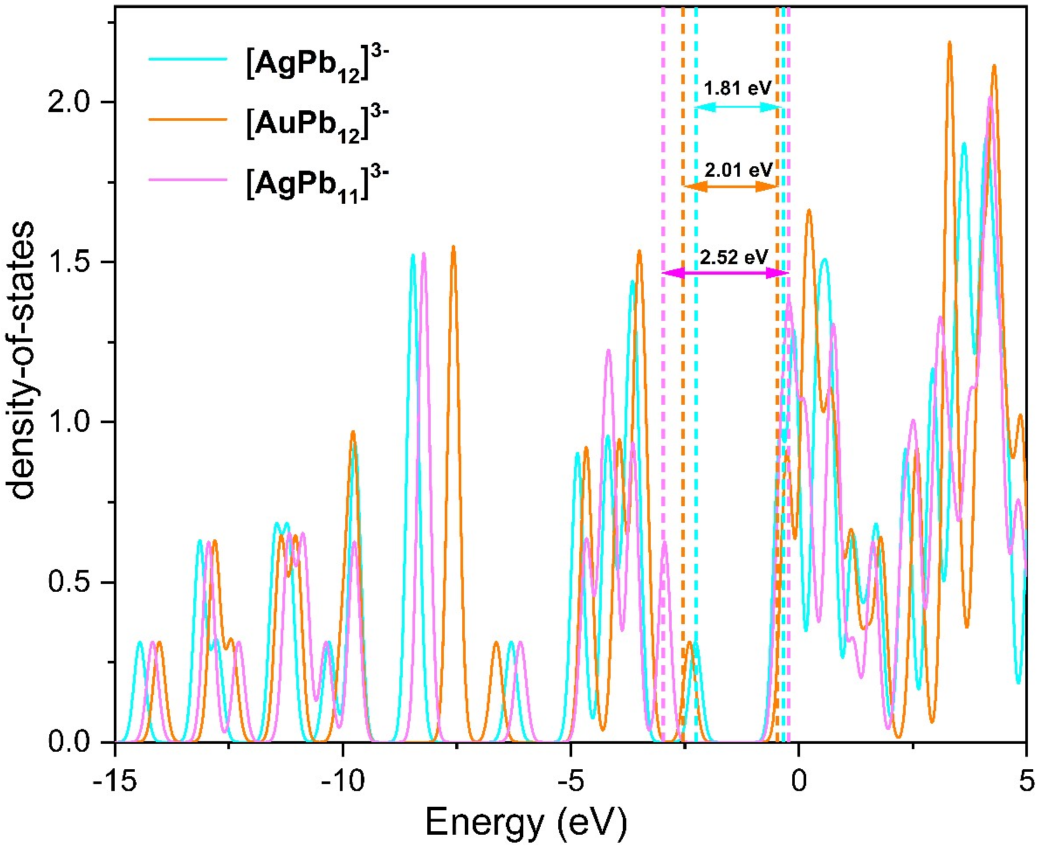

Figure S8. Total density of states (TDOS) for $[\mathrm{Ag@Pb}_{12}]^{3-}$ (blue), $[\mathrm{Au@Pb}_{12}]^{3-}$ (orange), and $[\mathrm{Ag@Pb}_{11}]^{3-}$ (pink). The Fermi level is at 0 eV.

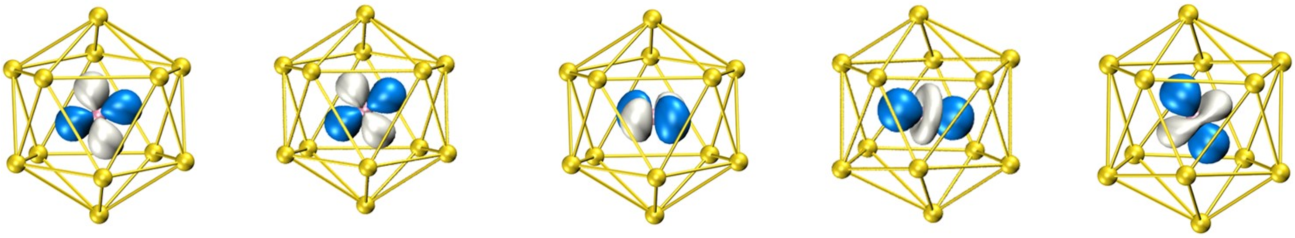

Five d-type lone pairs
ON = 1.99 - 1.98 |e|

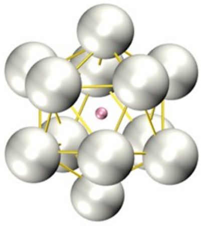

Twelve s-type lone pairs
ON = 1.90 |e|

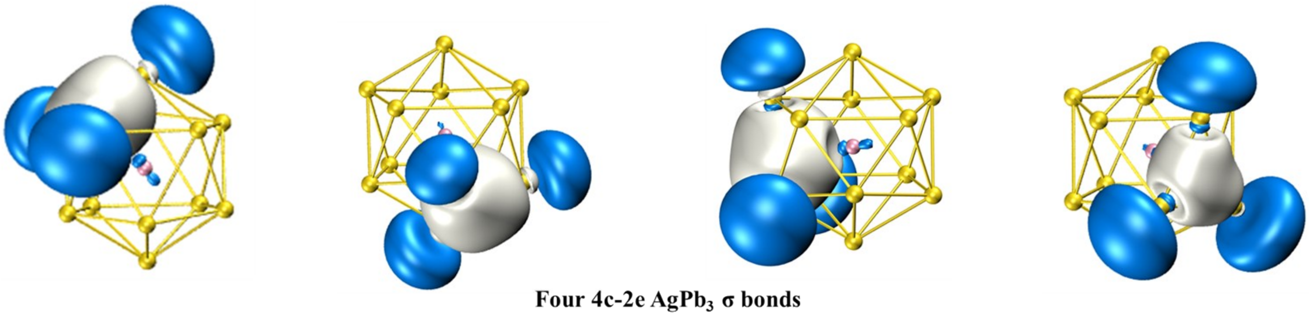

Four 4c-2e $AgPb_3$ σ bonds
ON = 1.80 - 1.90 |e|

Figure S9. AdNDP analysis of $[Ag@Pb_{12}]^{3-}$ cluster, ON represents occupancy number.

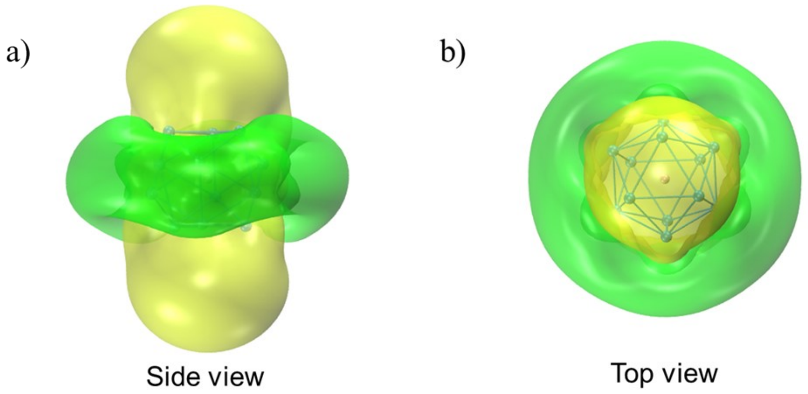

Figure S10. Iso-chemical shielding surface (ICSS) for $[Ag@Pb_{12}]^{3-}$ cluster. (a) Side views and (b) top views, where the yellow and green regions correspond to negative and positive ICSS values.

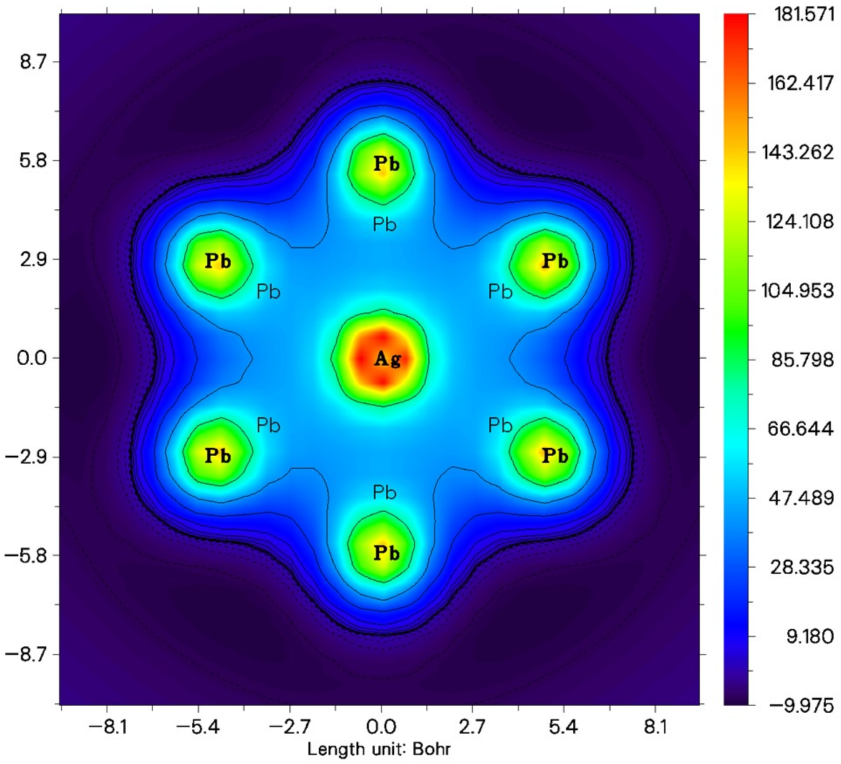

Figure S11. 2D ICSS contour map on the equatorial plane (through the central Ag atom), with shielding (red) and deshielding (blue) regions indicated.

References

[1] P. de Frémont, N.M. Scott, E.D. Stevens, et al., Synthesis of Well-Defined *N*-Heterocyclic Carbene Silver(I) Complexes. *Organometallics,* **2005**, *24*, 6301–6309.

[2] M. Halim, R.D. Kennedy, M. Suzuki, S.I. Khan, P.L. Diaconescu, Y. Rubin, *J. Am. Chem. Soc.,* 2011, **133**, 6841-6851.

[3] G. M. Sheldrick, SHELXT – Integrated space-group and crystal-structure determination. *Acta Crystallogr. Sect. A: Found. Adv.*, **2015**, *71*, 3-8.

[4] O. V. Dolomanov, L. J. Bourhis, R. J. Gildea, J. A. K. Howard, H. Puschmann, OLEX2: A complete structure solution, refinement and analysis program. *J. Appl. Crystallogr.*, **2009**, *42*, 339-341.

[5] A. L. Spek, Structure validation in chemical crystallography. *Acta Crystallogr. Sect. D: Biol. Crystallogr.*, **2009**, *65*, 148-155.

[6] S. Grimme, S. Ehrlich, L. Effect of the Damping Function in Dispersion Corrected Density Functional Theory. Goerigk, *J. Comput. Chem.*, **2011**, *32*, 1456–1465.

[7] C. Adamo, V. Barone, Toward reliable density functional methods without adjustable parameters: The PBE0 model, *J. Chem. Phys.* **1999**, *110*, 6158–6170.

[8] Pritchard BP, Altarawy D, Didier B et al, New basis set exchange: an open, up-to-date resource for the molecular sciences community. *J Chem Inf Model*. **2019**. *59*, 4814–4820.

[9] Lu, T.; Chen, F. Multiwfn: A multifunctional wavefunction analyzer. *J. Comput. Chem.* **2012**, *33*, 580–592.

[10] Lu, T. A comprehensive electron wavefunction analysis toolbox for chemists, Multiwfn. *J. Comput. Chem.* **2024**, *161*, 082503.

[11] Humphrey, W.; Dalke, A.; Schulten, K. VMD: Visual molecular dynamics. *J. Mol. Graph*. **1996**, *14*, 33–38.